Massive MIMO Channel Modeling - Extension of the COST 2100 Model

Gao, Xiang; Flordelis, Jose; Dahman, Ghassan; Tufvesson, Fredrik; Edfors, Ove

2015

EUROPEAN COOPERATION
IN THE FIELD OF SCIENTIFIC
AND TECHNICAL RESEARCH

EURO-COST

IC1004 TD(15)W1025
Barcelona, Spain
October 14-15, 2015

SOURCE: Department of Electrical and Information Technology
Lund University
Sweden

Massive MIMO Channel Modeling – Extension of the COST 2100 Model

Xiang Gao
Department of Electrical and Information Technology
Box 118, Lund University
SE-221 00 Lund
SWEDEN
Phone: + 46-46-222 90 17
Fax: + 46-46-12 99 48
Email: xiang.gao@eit.lth.se

Massive MIMO Channel Modeling – Extension of the COST 2100 Model

Xiang Gao, Jose Flordelis, Ghassan Dahman, Fredrik Tufvesson, Ove Edfors
Department of Electrical Information and Technology, Lund University, Sweden
E-mail: {firstname.lastname}@eit.lth.se

***Abstract*—As massive MIMO is currently considered a leading 5G technology candidate, channel models that capture important massive MIMO channel characteristics are urgently needed. In this paper we present an attempt for massive MIMO channel modeling based on measurement campaigns at 2.6 GHz in both outdoor and indoor environments, using physically-large arrays and with closely-spaced users. The COST 2100 MIMO channel model is adopted as a general framework. We discuss modeling approaches and scopes for massive MIMO, based on which we suggest extensions to the COST 2100 model. The extensions include 3D propagation, polarization, cluster behavior at the base station side for physically-large arrays, and multi-path component gain functions for closely-spaced users. Model parameters for these extensions in massive MIMO scenarios are reported. Initial validation against the measurements are also performed, which shows that the model is capable of reproducing the channel statistics in terms of temporal behavior of the user separability, singular value spread and sum-rate/capacity.**

***Index Terms*—Massive MIMO, channel modeling, COST 2100 MIMO channel model, channel measurements, 5G**

I. Introduction

Massive MIMO [1]–[4] is an emerging technology in wireless communications. With a large number of antennas at the base station, massive MIMO exploits a large number of spatial degrees of freedom in the propagation channels. It has been shown in both theory and experiments that massive MIMO can dramatically improve the spectral and transmit-energy efficiency of conventional MIMO by orders of magnitude [5]–[10]. With the potential of offering higher data rates and serving more users simultaneously, massive MIMO is thus considered as a leading 5G technology candidate [11]–[15]. When massive MIMO is brought from theory to practice, channel measurements were performed to evaluate massive MIMO in real propagation environments [6]–[10], and real-time massive MIMO testbeds are also being implemented [16]. In order to efficiently design massive MIMO system and test algorithms, channel models that include massive MIMO characteristics are now urgently needed.

So far, theoretical studies of massive MIMO are mostly done for channels with independent and identically distributed (i.i.d.) complex Gaussian coefficients, or based on correlative channel models, e.g., the Kronecker model. Channel models using an i.i.d. assumption do not consider channel correlations and power variations between users and between base station antennas, thus usually give more optimistic results than those obtained in real propagation channels. The Kronecker model is not suitable for physically-large arrays due to the assumption that the propagation at the transmitter and receiver sides are uncoupled, resulting in underestimation of the performance [17]. Another important aspect is the temporal behavior of the channels which is crucial for studying massive MIMO channel estimation, however, many correlative models are unable to model time-variation.

In this paper, we present an attempt for massive MIMO channel modeling based on measurement campaigns at 2.6 GHz in both outdoor and indoor environments. The COST 2100 MIMO channel model is adopted as a general framework. The COST 2100 model is a geometry-based stochastic channel model (GSCM), and inherently it is able to capture and model important massive MIMO channel characteristics, i.e., the user separability and the temporal behavior of the channel. Most importantly, the COST 2100 modeling approach and the developed model are in general not specific to massive MIMO only, which means they can be consistent in both the spatial and frequency domain, i.e., capturing the propagation behavior over a few wavelengths to hundreds of meters, and supporting lower frequencies as well as higher frequencies. We suggest extensions of the COST 2100 channel model for massive MIMO. The extensions include 3D propagation, polarization, cluster behavior at the base station side for physically-large arrays, and variability of multi-path component (MPC) gain for closely-spaced users.

The channel measurements on which we develop the massive MIMO channel model have been reported in [6]–[8], [18], [19]. The measurements were performed at 2.6 GHz and with 40 or 50 MHz bandwidth, using a physically-large linear array and a compact cylindrical array at the base station, both having 128 antenna elements. Scenarios with closely-spaced users were mea-

sured using the cylindrical array only, in an outdoor semi-urban environment emulating open exhibitions with a high user density, and in an indoor environment emulating crowded auditorium.

The rest of the paper is organized as follows. In Sec. II we review massive MIMO channel behavior that should be included in the new model, and we briefly discuss the limitations of current MIMO channel models. In Sec. III we discuss our modeling approach and scope, including model consistency and extensions to the COST 2100 model. We report initial parameters for the model extension in Sec. IV, and initial validation against measurements are presented in Sec. V. Finally in Sec. VI we summarize our work and draw conclusions.

II. Review of Massive MIMO Channel Behavior

Massive MIMO channel behavior including spherical wavefronts and large-scale fading over physically-large arrays have been reported in [18], [20]. With closely-spaced users, massive MIMO channel characteristics have been observed and presented in [8], [19]. Here we briefly review these new features of massive MIMO channels that have to be modeled, as compared to conventional MIMO channels.

A. New Features of Massive MIMO Channels

Compared with conventional MIMO channel, the radio channel of a massive MIMO system is of course the same, independent of system and antenna configuration used, but some propagation effects become more pronounced or more important when using physically-large arrays, when using many antenna elements at the base station, and when having many closely-located users. These effects are important and we need to capture detailed behavior that can explain, e.g., user separability, temporal behavior, as well as the possibilities for significant increases in spectral and transmit-energy efficiency. Among the important specific propagation effects for massive MIMO can be mentioned noticeable spherical wavefronts, variations of statistics over physically-large arrays, and the limited lifetime of individual MPCs when a user is moving.

When physically-large arrays are used at the base station, users or significant scatterers may be located inside the Rayleigh distance of the array, e.g., the 7.4 m linear array in [6] gives a Rayleigh distance of about 950 m. Plane-wave assumption does not hold for large arrays, and spherical wavefronts are observed over the array [10]. The spherical wavefronts are important to model because then not only directions to users and scatterers are important, but also the distances to scatterers and users. The inherent beamforming capability of massive MIMO makes it possible to focus the signal energy to a specific point in the environment rather than just in a certain direction. Furthermore, if two users are in the same direction but at different distances from the base station, the spherical wavefronts can make it possible to separate those users, also in line-of-sight (LOS) [21]. This is typically not the case for conventional MIMO using smaller arrays.

The variations in statistics of the received signal from a specific user over physically-large arrays also contributes to the ability of user separation. The variations include, e.g., received signal power, angular power spectra, as well as power delay profile between different antenna elements [10], also in cases where they have identical antenna patterns aimed in the same direction. Variations of the angular power spectra can be characterized by the so-called spatial fingerprints [6]. The large-scale fading over the array can also be crucial for massive MIMO performance, as the antennas do not contribute equally to the performance [7].

When having many closely-spaced users, e.g., in a scenario with a crowd of people, the limited lifetime of individual MPCs is another important effect to consider when analyzing user separability. In conventional MIMO channel models, all the scatterers in a cluster are visible from all positions in the visibility region of the cluster. In practice this is, however, not the case. Each of the MPCs typically has a limited area inside the visibility region where they can be seen. Clusters provide a very effective way of modeling antenna correlation for a single user, but our observations show that conventional MIMO models tend to overestimate correlation between users in massive MIMO systems.

Other propagation effects that become important in massive MIMO scenarios include 3D propagation, because arrays with a large number of antennas may span in azimuth as well in elevation depending on the array geometry.

B. Current MIMO Channel Models

Among MIMO channel models, the GSCMs provide a natural way to capture time-variation and describe correlation effects between users and between antenna elements in a straightforward way through the concept of clusters and their visibility regions.

Within the group of GSCMs there are two basic approaches having the same origin (the COST 259 model): the COST 2100 approach and the WINNER approach. In the COST 2100 [22] approach, the scatterers have fixed physical positions in the simulated environment, whereas in the WINNER [23] approach the channel simulation is based on angles to the scatterers. From a massive MIMO perspective the latter has the drawback that the angles vary as long as we are not in the far field of the array;

hence we need to include this in the model. Due to this reason and since we aim for a consistent model showing realistic correlations between users in a massive MIMO context, we use the COST 2100 modeling approach where the clusters and scatterers are described by their physical locations rather than their directions in the simulation area. The model extensions we propose are in general, not specific to massive MIMO only, as they realistically represent physical propagation mechanisms when taking wireless communication beyond the conventional cellular scenario with one or several base stations. The concepts introduced should, e.g., be useful also for peer-to-peer channels or when developing models for radio-based positioning. In this paper, however, we focus on the massive MIMO scenario with one base station equipped with many antennas and several users having mobile terminals with one or a few antennas.

It should also be mentioned that there are theoretical geometrical model proposals in the literature, e.g., in [24]. As we aim for a model connected to a physical environment those models are out of scope of our investigation, though these theoretical models can provide useful insights into, e.g., correlation characteristics. Ray-tracing based investigations and models can also provide useful insights for system design and performance evaluation, but those models rely heavily on a deterministic geometry and thus also out of scope of our investigation here.

III. Modeling Approach and Scope

In this section we introduce our modeling approach and scope, and suggest the extensions to the COST 2100 channel model.

A. Model Consistency

As explained above, the COST 2100 model is adopted in this work as a general framework, since it has the required flexibility to model different aspects of massive MIMO channels. Besides the requirement of capturing channel behavior in different spatio-temporal, angular, and delay domains, the developed channel model should also be consistent in both the spatial and frequency domains.

In the spatial domain, the channel model should be able to capture the propagation behavior over small distances in the range of a wavelength to very large distances (hundreds of meters), for both the user side and the base station side. The model should cover the cases where user terminals are closely-spaced to the cases where user terminals are far separated and the cases where the base station array is physically small to the cases where it is physically large. The consistency in the spatial domain makes it possible to compare massive MIMO with conventional MIMO.

In the frequency domain, the channel model should support low frequencies (below 6 GHz) as well as high frequencies (above 6 GHz). The consistency in the frequency domain has become ever more important due to the trend of 5G communications toward using the higher frequency band, i.e., the 6-100 GHz band. The COST 2100 model can meet the consistency requirement in both the spatial and frequency domains, as discussed above. We, however, limit the efforts here to the case below 6 GHz.

B. Extension of the COST 2100 Channel Model

The extensions are based on the performed measurement campaigns, and modeling aspects for physically-large arrays and closely-spaced users are implemented. In the case of having limitations preventing us from extracting some parameters of interest based on our measurement data, these parameters are implemented based on the 3GPP and WINNER channel models [23], [25]. The implemented extensions for the COST 2100 model are detailed in the sequel.

1) 3D Extension: Supporting elevation angles for the MPCs is crucial in capturing the behavior of the channel especially when base station arrays span in both azimuth and elevation. Besides that, the proximity of the base station and/or the user terminals to the interacting objects in the environment makes the effect of the elevation angles more pronounced. Therefore, the propagation in the COST 2100 model simulation has been extended to 3D, by including parameters such as intra-cluster angular spread in elevation for both the base station and the user side. Due to limitations in extracting these parameters based on our measurements, the parameter values of cluster angular spreads in elevation are thus adopted from the 3GPP 3D model [25].

2) Polarization Extension: One of the main results discussed in [8] is the significant effect of the polarization on massive MIMO performance when serving closely-spaced users. Both vertical and horizontal-polarized antennas at the base station are useful for separating the users. This is of great importance since the polarization at the user side is usually dual but unknown when having the hand and head effect on the antenna pattern. We also gain from the user diversity due to the difference in user polarizations and patterns. Therefore, the COST 2100 model has been extended by including the polarization for the MPCs, i.e., in a single MPC, how much energy is from co-polarization (vertical to vertical and horizontal to horizontal), and how much is from cross-polarization (vertical to horizontal and horizontal to vertical).

In our measurements, however, due to lack of the polarization information at the user side, we adopt the cross polarization ratio (XPR) parameters reported in the

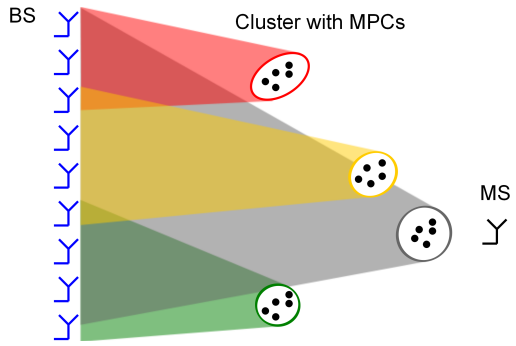

Fig. 1. An illustration of the extension of cluster visibility regions to the base station side [26].

WINNER II models. There, XPR for each MPC follows log-normal distribution $\kappa = 10^{\frac{X}{10}}$, where $X \sim N(\mu, \sigma)$. For indoor office (A1) scenario, the mean $\mu = 11$ dB for LOS and $\mu = 10$ dB for NLOS, and the standard deviation $\sigma = 4$ dB. For large indoor hall hotspot (B3), $\mu = 9$ dB for LOS and $\mu = 6$ dB for NLOS, $\sigma = 4$ dB and $\sigma = 3$ dB for LOS and NLOS, respectively. For urban micro-cell (B1), $\mu = 9$ dB for LOS and $\mu = 8$ dB for NLOS, and $\sigma = 3$ dB.

3) Extension for Physically-Large Arrays: Dedicated measurement campaigns were performed for the scenarios with physically-large arrays at the base station [6], [18]. It has been observed that spherical wavefronts and large-scale fading are experienced across the large array. In order to capture the effect of having a physically-large array and be compatible with the conventional model, the simulation area at the base station side is extended to several meters, and the cluster visibility region at the base station side is introduced, see Fig. 1. A cluster thus has two visibility regions, one at the user side (MS-VR) and one at the base station side (BS-VR), and the cluster contributes in the channel between a user and a base station antenna only when the user is within its MS-VR and the base station antenna is within its BS-VR. Based on the measurements, the size of BS-VRs and the power variation of a cluster within its BS-VR, i.e., the visibility gain, have been modeled and implemented. The number of clusters can be more than in conventional MIMO channels, since physically-large arrays "see" the channel more in the spatial domain. This extension naturally captures the effect of the spherical wavefronts.

The extension for physically-large arrays is consistent with physically-compact arrays that a whole array is within the same BS-VR. This allows direct comparison of physically-large and compact arrays in the simulation.

4) Extension for Closely-Spaced Users: Different measurement campaigns were performed for the scenarios with closely-located users, in both outdoor and indoor environments. The users were confined within a small area, i.e., 5 m diameter circle, therefore, we assume that all users stay within the same cluster visibility regions. When a user is moving within this confined area, the effects of changing its position, orientation and antenna tilt and the effect of the crowd around the user are captured as follows.

When a user is moving within a cluster visibility region, it will result in varying the power contribution of each MPC. This makes individual MPCs to have different patterns describing their contribution to the channel at each user position. This effect is captured by introducing MPC gain functions that have a symmetric Gaussian shape. Each MPC has its own gain function and it has a peak location randomly distributed within the corresponding cluster visibility region. The gain is thus determined by the distance d between the peak location and the user location,

$$g_{\mathrm{MPC}}(d) = \exp\left(-\frac{d^2}{2\sigma_g^2}\right), \tag{1}$$

where the standard deviation σ_g determines the width of the gain function and controls the variability of the MPC gain. From our preliminary observation, the lifetime of MPCs is about 2 m, we therefore set $\sigma_g = 2.37$ that corresponds to 3 dB power decay when $d = 2$ m.

The number of MPCs per cluster $N_{\mathrm{MPC}}^{\mathrm{total}}$, the average number of effective MPCs per cluster $N_{\mathrm{MPC}}^{\mathrm{effective}}$, the radius of cluster visibility region R_c and the radius of 3-dB power decay of MPC gain function r_g fulfill the following relation

$$N_{\mathrm{MPC}}^{\mathrm{total}} = N_{\mathrm{MPC}}^{\mathrm{effective}} \frac{R_c^2}{r_g^2}. \tag{2}$$

According to the conventional models (COST 2100 and WINNER II), we choose the average number of effective MPCs per cluster to be 16. Hence, with $R_c = 10$ m and $r_g = 2$ m, the total number of MPCs per cluster is 400. The large amount of MPCs with weak power possibly can be regarded as diffuse multipath components (DMC). Backward compatibility with the conventional model can be achieved by setting a large standard deviation for the gain functions.

The user antenna pattern that includes the interaction between the terminal antenna and the user body can capture the effect of changing the orientation, the tilt of the antenna and the shadowing by the users. The shadowing effect due to the crowd around the users possibly can be modeled as extra absorbing objects dropped within the simulation area. This, however, needs further investigations, so far we do not include absorbing objects in the model.

IV. Model Parameters

We report the initial parameters for the model extensions discussed above.

TABLE I
PARAMETERS OF THE COST 2100 MODEL EXTENSION FOR PHYSICALLY-LARGE ARRAYS, EXTRACTED FROM THE 2.6 GHZ MEASUREMENTS, SEMI-URBAN OUTDOOR.

Parameter	LOS group	NLOS group
Total number of clusters		
r_N	-	2.43
p_N	-	0.16
Length of BS-VR [m]		
μ_α	-	0.7
σ_α	-	2
Slope of BS-VR gain [dB/m]		
μ_s	-	0
σ_s	-	0.9
Cluster power decay factor		
k_τ [dB/μs]	27.83	42.98
Cluster cut-off delay		
τ_{B} [μs]	0.87	0.91
Cluster shadowing factor		
σ_{S} [dB]	5.84	7.55
Number of MPCs per cluster		
N_{MPC}	30	31
Cluster delay spread		
m_τ [μs]	0.15	0.14
S_τ [dB]	3.20	2.85
Cluster angular spread		
$m_{\psi_{\mathrm{BS}}}$ [deg]	11.04	6.96
$S_{\psi_{\mathrm{BS}}}$ [dB]	2.93	2.39
Cluster spread cross-correlation		
$\rho_{\psi_{\mathrm{BS}}\tau}$	0.27	0.42
$\rho_{\psi_{\mathrm{BS}}\sigma_{\mathrm{S}}}$	0.09	0.04
$\rho_{\tau\sigma_{\mathrm{S}}}$	0.35	-0.09
LOS power factor		
$\mu_{K_{\mathrm{LOS}}}$	5.19	-
$\sigma_{K_{\mathrm{LOS}}}$ [dB]	3.47	-

A. Scenario with Physically-Large Arrays

In Table I, we list the parameters of the model extension for physically-large arrays. Details of the parameter extraction can be found in [18], [20], [26].

B. Scenario with Closely-Spaced Users

In Table II, we list the initial parameters for the model extension with closely-spaced users. As marked in the table, some parameter values are adopted from a 300 MHz outdoor measurements for the COST model, and some are adopted from the 3GPP 3D channel model and the WINNER II channel models.

V. VALIDATION AGAINST MEASUREMENTS

We validate the model extension for closely-spaced users in LOS scenarios. In order to validate the concept and use of MPC gain functions, in the simulation we place the clusters at the same positions and with the same cluster spreads as in the measurements. Randomness is obtained through cluster shadowing, MPC distribution within clusters, and LOS K-factors, etc. We simulate

TABLE II
PARAMETERS OF THE COST 2100 MODEL EXTENSION FOR CLOSELY-SPACED USERS, EXTRACTED FROM 2.6 GHZ MEASUREMENTS, SEMI-URBAN OUTDOOR.

Parameter	LOS scenario	NLOS scenario
Number of far clusters		
N_{C}	15	14
Radius of cluster visibility region		
R_{C} [m]	10	10
Radius of cluster transition region		
T_{C} [m]	2	2
Number of MPCs per cluster		
N_{MPC}	400	400
Cluster power decay factor		
k_τ [dB/μs]	79.6	20
Cluster cut-off delay		
τ_{B} [μs]	1.7	1.7
Cluster shadowing		
σ_{S} [dB]	5.8	5
Cluster delay spread		
m_τ [μs]	0.02	0.06
S_τ [dB]	0.01	0.01
Cluster angular spread in azimuth (at BS)		
$m_{\psi_{\mathrm{BS}}}$ [deg]	8.5	9.8
$S_{\psi_{\mathrm{BS}}}$ [dB]	1.9	2.2
Cluster angular spread in elevation (at BS)		
$m_{\theta_{\mathrm{BS}}}$ [deg]	7.0	8.9
$S_{\theta_{\mathrm{BS}}}$ [dB]	1.9	1.9
Cluster angular spread in azimuth (at MS)[1]		
$m_{\psi_{\mathrm{MS}}}$ [deg]	14.8	19
$S_{\psi_{\mathrm{MS}}}$ [dB]	2.68	2.03
Cluster angular spread in elevation (at MS)[2]		
$m_{\theta_{\mathrm{MS}}}$ [deg]	4	7.6
$S_{\theta_{\mathrm{MS}}}$ [dB]	1.6	1.6
Cluster spread cross-correlation		
$\rho_{\tau\sigma_{\mathrm{S}}}$	-0.5	-0.4
$\rho_{\psi_{\mathrm{BS}}\sigma_{\mathrm{S}}}$	-0.8	-0.8
$\rho_{\theta_{\mathrm{BS}}\sigma_{\mathrm{S}}}$	-0.8	-0.7
$\rho_{\psi_{\mathrm{BS}}\tau}$	0.6	0.4
$\rho_{\theta_{\mathrm{BS}}\tau}$	0.4	0.2
$\rho_{\psi_{\mathrm{BS}}\theta_{\mathrm{BS}}}$	0.7	0.7
Radius of LOS visibility region[1]		
R_{L} [m]	343	-
Radius of LOS transition region[1]		
T_{L} [m]	93	-
LOS power factor		
$\mu_{K_{\mathrm{LOS}}}$ [dB]	2.8	-
$\sigma_{K_{\mathrm{LOS}}}$ [dB]	0.8	-
XPR[3]		
μ_{XPR} [dB]	9	8
σ_{XPR} [dB]	3	3
MPC gain function		
σ_g	2.37	2.37

[1]Parameter values adopted from the 300 MHz outdoor measurements for the COST 2100 model [27].
[2]Parameter values adopted from the 3GPP 3D channel model [25].
[3]Parameter values adopted from the WINNER II channel models [23].

the user movements in straight lines but with random rotations (between $-\pi$ to π) of user antenna patterns in order to emulate the rotation of users during the movements. The user antenna pattern we use in the simulation is a measured pattern in the hand of an upper body phantom. The base station antenna pattern is the measured cylindrical array antenna pattern. In the validation we also add artificial noise to the simulated channels, according to the signal-to-noise ratio (SNR) in the measurements, i.e., about 16-20 dB. We compare the simulated channels with the measured channels in terms of user separability, linear precoding sum-rates as well as temporal behavior.

As explained earlier, the closely-spaced users can be spatially separated because they "see" different MPCs, and this is modeled by the MPC gain function. We validate this model extension by evaluating the singular value spreads and the achieved sum-rates in the simulated channels, as compared with those in the measured channels. The model should also be consistent in spatial domain and be able to capture propagation behavior from small distances that are less than half-wavelength to distances that are at least a few wavelengths. We therefore validate the temporal behavior of the simulated channels from 0.01 m to 1 m through the auto-correlation functions when users are moving. We discuss these validation in the following.

A. User Orthogonality

As shown in Fig. 2, the singular value spreads of the simulated channels match well with those of the measured channels. However, in the simulated channels, the singular value spreads have larger variations. That means, in the simulated channels, we obtain relatively low singular value spreads as well as relatively high singular value spreads. The reason could be lack of statistics in the simulations due to 1) number of simulations, 2) randomness in user movements, 3) diversities in user antenna patterns. We also see similar trends that the singular value spreads become smaller when increasing the number of antennas, and the difference is very small between the cases of 64 and 128 antennas. The simulation could be improved by introducing more randomness in user movements, and adding crowd effect to the user antenna patterns. This has been left for future work.

B. Linear Precoding Sum-Rates

Comparing the CDFs of MRC and ZF sum-rates in the simulated and measured channels in Fig. 3, we clearly see larger variations in the simulated channels. This is more obvious in the ZF sum-rates than in the MRC sum-rates. It can be explained by the fact that the ZF

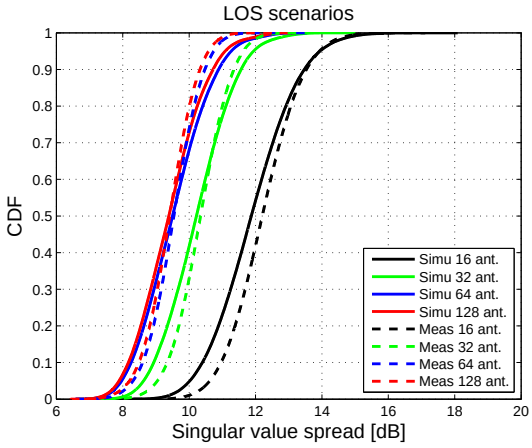

Fig. 2. Singular value spreads of the simulated channels and measured channels.

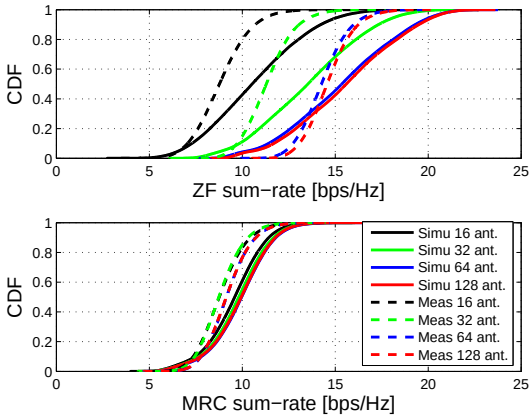

Fig. 3. Downlink sum-rates by ZF and MRC in the simulated channels and measured channels, when the average interference-free SNR at the users is 10 dB.

precoding is more sensitive to the user correlation than the MRC. Again, it could be due to lack of randomness and statistics in the simulation.

C. Temporal Behavior

The temporal behavior of the simulated and measure channels, in terms of auto-correlation when one user is moving, are shown in Fig. 4. The auto-correlation is averaged over different users, snapshots and frequencies. The correlation coefficient $c(\Delta_t)$ is calculated as below,

$$c(\Delta_t) = \frac{1}{L}\sum_{\ell=1}^{\ell=L}\frac{1}{K}\sum_{k=1}^{k=K}\frac{1}{T}\sum_{t=1}^{t=T}\left|\frac{\mathbf{h}_{t,k,\ell}\mathbf{h}_{t+\Delta_t,k,\ell}^{H}}{\|\mathbf{h}_{t,k,\ell}\|\,\|\mathbf{h}_{t+\Delta_t,k,\ell}\|}\right|, \tag{3}$$

where $\mathbf{h}_{t,k,\ell}$ is the $1\times M$ channel vector, M is the number of BS antennas, and t, k and ℓ represent snapshots, users and frequencies, respectively. Note that

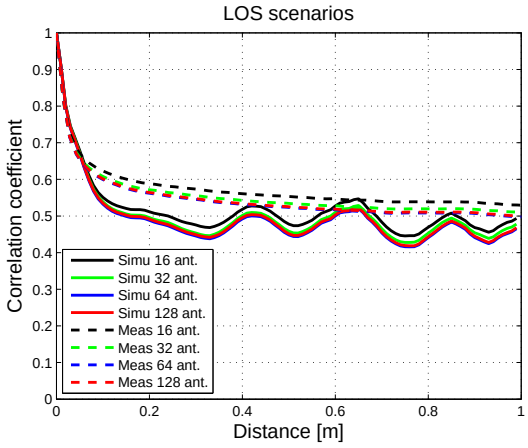

Fig. 4. Auto-correlation in distance of the simulated channels and measured channels.

the averaging is performed on the amplitudes of the correlation coefficients in each realization. We see in Fig. 4 that from 0.01 m to 1 m the auto-correlation in the simulated channels matches with that in the measured channels, although the auto-correlation is slightly lower and the variation is larger in the simulated channels. This indicates that with the model extension we are able to capture the temporal behavior of the channels in a small distance.

VI. Summary and Conclusions

Based on the massive MIMO channel measurements at 2.6 GHz, we have proposed and implemented a backwards compatible extension of the COST 2100 channel model for massive MIMO. The extension includes:

- 3D propagation, as the large arrays at the base station envisioned most likely will have the ability to resolve clusters both in azimuth and elevation;
- Polarization, as dual-polarization at the base station antennas will help to spatially separate the users;
- Cluster behavior at the base station, as spherical wavefronts and large-scale fading can be experienced over physically-large arrays;
- Individual gain functions of individual MPCs, as individual MPCs tend not to be visible in the entire cluster visibility region.

The initial validation showed that the proposed and implemented model extensions are capable of reproducing the channel statistics in terms of user separability, linear precoding sum-rates and temporal behavior. The COST 2100 model extension for massive MIMO can be a valuable input for 5G channel modeling. Future work include parametrization of more scenarios and more validations of the model.

Acknowledgement

The authors would like to acknowledge the support from ELLIIT - an Excellence Center at Linköping-Lund in Information Technology, the Swedish Research Council (VR), and the Swedish Foundation for Strategic Research (SSF). The research leading to these results has received funding from the European Union Seventh Framework Programme (FP7/2007-2013) under grant agreement n° 619086 (MAMMOET).

References

[1] F. Rusek, D. Persson, B. K. Lau, E. G. Larsson, T. L. Marzetta, O. Edfors, and F. Tufvesson, "Scaling up MIMO: Opportunities and challenges with very large arrays," *IEEE Signal Processing Magazine*, vol. 30, no. 1, pp. 40–60, Jan. 2013.

[2] E. Larsson, O. Edfors, F. Tufvesson, and T. Marzetta, "Massive MIMO for next generation wireless systems," *IEEE Communications Magazine*, vol. 52, no. 2, pp. 186–195, Feb. 2014.

[3] T. Marzetta, "Massive MIMO: An introduction," *Bell Labs Technical Journal*, vol. 20, pp. 11–22, 2015.

[4] E. Björnson, E. G. Larsson, and T. L. Marzetta, "Massive MIMO: 10 myths and one grand question," Mar. 2015, arXiv:1503.06854.

[5] H. Q. Ngo, E. G. Larsson, and T. L. Marzetta, "Energy and spectral efficiency of very large multiuser mimo systems," *IEEE Transactions on Communications*, vol. 61, no. 4, pp. 1436–1449, Apr. 2013.

[6] X. Gao, O. Edfors, F. Rusek, and F. Tufvesson, "Massive MIMO performance evaluation based on measured propagation data," *IEEE Transactions on Wireless Communications*, vol. 14, no. 7, pp. 3899–3911, July 2015.

[7] X. Gao, O. Edfors, F. Tufvesson, and E. G. Larsson, "Massive MIMO in real propagation environments: Do all antennas contribute equally?" *IEEE Trans. Commun.*, 2015.

[8] J. Flordelis, X. Gao, G. Dahman, F. Rusek, O. Edfors, and F. Tufvesson, "Spatial separation of closely-spaced users in measured multi-user massive MIMO channels," in *2015 IEEE International Conference on Communications (ICC)*, June 2015.

[9] J. Hoydis, C. Hoek, T. Wild, and S. ten Brink, "Channel measurements for large antenna arrays," in *2012 International Symposium on Wireless Communication Systems (ISWCS)*, Aug. 2012, pp. 811–815.

[10] S. Payami and F. Tufvesson, "Channel measurements and analysis for very large array systems at 2.6 GHz," in *2012 6th European Conference on Antennas and Propagation (EUCAP)*, Mar. 2012, pp. 433–437.

[11] J. Andrews, S. Buzzi, W. Choi, S. Hanly, A. Lozano, A. Soong, and J. Zhang, "What will 5G be?" *IEEE Journal on Selected Areas in Communications*, vol. 32, no. 6, pp. 1065–1082, June 2014.

[12] F. Boccardi, R. Heath, A. Lozano, T. Marzetta, and P. Popovski, "Five disruptive technology directions for 5G," *IEEE Communications Magazine*, vol. 52, no. 2, pp. 74–80, Feb. 2014.

[13] V. Jungnickel, K. Manolakis, W. Zirwas, B. Panzner, V. Braun, M. Lossow, M. Sternad, R. Apelfröjd, and T. Svensson, "The role of small cells, coordinated multipoint, and massive MIMO in 5G," *IEEE Communications Magazine*, vol. 52, no. 5, pp. 44–51, May 2014.

[14] A. Osseiran, F. Boccardi, V. Braun, K. Kusume, P. Marsch, M. Maternia, O. Queseth, M. Schellmann, H. Schotten, H. Taoka, H. Tullberg, M. Uusitalo, B. Timus, and M. Fallgren, "Scenarios for 5G mobile and wireless communications: the vision of the METIS project," *IEEE Communications Magazine*, vol. 52, no. 5, pp. 26–35, May 2014.

[15] C.-X. Wang, F. Haider, X. Gao, X.-H. You, Y. Yang, D. Yuan, H. Aggoune, H. Haas, S. Fletcher, and E. Hepsaydir, "Cellular architecture and key technologies for 5G wireless communication networks," *IEEE Communications Magazine*, vol. 52, no. 2, pp. 122–130, Feb. 2014.

[16] J. Vieira, S. Malkowsky, K. Nieman, Z. Miers, N. Kundargi, L. Liu, I. Wong, V. Owall, O. Edfors, and F. Tufvesson, "A flexible 100-antenna testbed for massive MIMO," in *Globecom Workshops (GC Wkshps), 2014*, Dec. 2014, pp. 287–293.

[17] X. Gao, M. Zhu, F. Rusek, F. Tufvesson, and O. Edfors, "Large antenna array and propagation environment interaction," in *2014 48th Asilomar Conference on Signals, Systems and Computers (ASILOMAR)*, Nov. 2014.

[18] X. Gao, F. Tufvesson, and O. Edfors, "Massive MIMO channels - measurements and models," in *2013 47th Asilomar Conference on Signals, Systems and Computers (ASILOMAR)*, Nov. 2013.

[19] "Mami channel characteristics: Measurement results," Lund University, Tech. Rep. ICT-619086-D1.2, June 2015.

[20] X. Gao, F. Tufvesson, O. Edfors, and F. Rusek, "Channel behavior for very-large MIMO systems - initial characterization," in *COST IC1004, Bristol, UK*, Sep. 2012.

[21] Z. Zhou, X. Gao, J. Fang, and Z. Chen, "Spherical wave channel and analysis for large linear array in LoS conditions," in *2015 IEEE Global Telecommunications Conference (GLOBECOM) Workshop on Massive MIMO From theory to practice*, 2015.

[22] L. Liu, C. Oestges, J. Poutanen, K. Haneda, P. Vainikainen, F. Quitin, F. Tufvesson, and P. Doncker, "The COST 2100 MIMO channel model," *IEEE Wireless Communications*, vol. 19, no. 6, pp. 92–99, December 2012.

[23] P. Kyösti, J. Meinilä, L. Hentilä, X. Zhao, T. Jämsä, C. Schneider, M. Narandzić, M. Milojević, A. Hong, J. Ylitalo *et al.*, "WINNER II channel models," 2008.

[24] S. Wu, C.-X. Wang, E.-H. Aggoune, M. Alwakeel, and Y. He, "A non-stationary 3-D wideband twin-cluster model for 5G massive MIMO channels," *IEEE Journal on Selected Areas in Communications*, vol. 32, no. 6, pp. 1207–1218, June 2014.

[25] "Study on 3D channel model for LTE," 3GPP, Tech. Rep. TR 36.873 V12.1.0, 2015.

[26] X. Gao, M. Zhu, F. Tufvesson, F. Rusek, and O. Edfors, "Extension of the COST 2100 channel model for massive MIMO," in *COST IC1004, Dublin, Ireland*, January 2015.

[27] M. Zhu, G. Eriksson, and F. Tufvesson, "The COST 2100 channel model: Parameterization and validation based on outdoor MIMO measurements at 300 MHz," *IEEE Transactions on Wireless Communications*, vol. 12, no. 2, pp. 888–897, February 2013.